Biosensors and Bioelectronics 311 (2026) 118943



Contents lists available at ScienceDirect

Biosensors and Bioelectronics

journal homepage: www.elsevier.com/locate/bios



# Smartphone-integrated RPA-CRISPR/Cas12a detection system with microneedle sampling for early point-of-care diagnosis of potato late blight

Jiangnan Zhao [a,b], Hanbo Xu [a,b], Shifang Fei [c], Cifu Xu [a,b], Wenlong Yin [a,b], Qingshan Wei [d], Jianhan Lin [a,b], Gang Liu [a,b], Shilun Feng [c], Fang Gao [e,*], Yan Wang [a,b,**]

[a] Key Laboratory of Smart Agriculture Systems, Ministry of Education, College of Information and Electrical Engineering, China Agricultural University, Beijing, 100083, China
[b] Key Laboratory of Agricultural Information Acquisition Technology, Ministry of Agriculture and Rural Affairs of China, College of Information and Electrical Engineering, China Agricultural University, Beijing, 100083, China
[c] State Key Laboratory of Transducer Technology, Shanghai Institute of Microsystem and Information Technology, Chinese Academy of Sciences, Shanghai, 200050, China
[d] Department of Chemical and Biomolecular Engineering, North Carolina State University, 911 Partners Way, Campus Box 7905, Raleigh, NC, 27695, USA
[e] Institute of Energy Materials Science, University of Shanghai for Science and Technology, Shanghai, 200093, China

ARTICLE INFO

*Keywords:*
CRISPR/Cas12a
Microneedle
RPA
Smartphone
Point-of-care testing
Potato late blight

ABSTRACT

Potato late blight, caused by the oomycete pathogen *Phytophthora infestans* (*P. infestans*), is one of the most devastating diseases threatening global potato production. Conventional plant disease detection methods rely on a labor-intensive and time-consuming workflow and require bulky and expensive benchtop equipment, limiting their in-field applications. Here, we report a portable RPA-CRISPR/Cas12a-based diagnostic platform integrated with a polyvinyl alcohol (PVA) microneedle (MN) patch, which allows rapid in-field sampling, and smartphone-based fluorescence acquisition and analysis to detect *P. infestans* in potato at the early stage. The PVA MN enables leaf sampling rapidly within 1 min, and yields efficient DNA extraction of 56.3 ± 4.2 ng/mg, which is ~3-fold higher than the traditional CTAB method (18.1 ± 2.1 ng/mg). The RPA-CRISPR/Cas12a isothermal assay achieved specific detection of *P. infestans* with no cross-reactivity against closely-related species *Phytophthora sojae* or *Phytophthora capsici*. The smartphone-based point-of-care test (POCT) system demonstrates a detection limit of 4 pg/μL for *P. infestans* genomic DNA, which is comparable to that acquired with commercial laboratory equipment. The method enables early-stage diagnosis of potato late blight as early as Day 2 post-inoculation, with detection rates of 37.5% on Day 2 and 75% on Day 3, prior to the development of visible symptoms on leaves. This portable "sample-to-result" platform provides a promising strategy for rapid, field-deployable early diagnosis and surveillance of plant disease.

## 1. Introduction

Late blight of potato, caused by the oomycete *Phytophthora infestans* (*P. infestans*), is one of the most destructive diseases threatening global potato production (Fry et al., 2015; Kong et al., 2020). Historically, it triggered the Irish Great Famine in the 1840s, leading to millions of deaths and mass migration (Anderson et al., 2004; Haas et al., 2009; Tang et al., 2023). *P. infestans* infects potato leaves, tubers, and stems, spreads rapidly under cool and humid conditions and is often referred to as the "cancer of potatoes". Once symptoms appear, entire potato fields can be devastated within weeks (Austin Bourke, 1964; Fry, 2008; Ristaino et al., 2020). Therefore, an early and accurate field-deployable detection method is necessary and crucial for effective management of late blight.

However, early detection is hampered by the limitations of conventional DNA extraction methods. Traditional plant nucleic acid extraction protocols, such as the cetyltrimethylammonium bromide (CTAB) method, are labor-intensive, time-consuming, and require specialized laboratory equipment and trained personnel, limiting their applicability for rapid on-site diagnosis. Recent advances in microneedle (MN)

* Corresponding author.
** Corresponding author. Key Laboratory of Smart Agriculture Systems, Ministry of Education, College of Information and Electrical Engineering, China Agricultural University, Beijing, 100083, China.
*E-mail addresses:* fgao@usst.edu.cn (F. Gao), yanwang@cau.edu.cn (Y. Wang).

https://doi.org/10.1016/j.bios.2026.118943
Received 19 January 2026; Received in revised form 4 June 2026; Accepted 17 June 2026
Available online 20 June 2026
0956-5663/© 2026 Elsevier B.V. All rights are reserved, including those for text and data mining, AI training, and similar technologies.

technology have demonstrated their potential in biomedical research for rapid, minimally invasive sampling, drug delivery and biosensing from human tissues and bodily fluids (Hung et al., 2025; Wang et al., 2025; B. Zheng et al., 2024; M. Zheng et al., 2024).

MN patches are typically fabricated from hydrophilic polymers and consist of arrays of microscale needles capable of penetrating biological tissues in a minimally invasive manner (Wu and Liu, 2026). Upon insertion, the microneedles mechanically disrupt cell membranes, facilitating the release of intracellular DNA or RNA, while the polymer matrix absorbs interstitial fluid, capturing and concentrating nucleic acids on the needle tips. These features enable direct nucleic acid isolation without conventional grinding, centrifugation, or complex purification procedures, demonstrating the huge potential for rapid, field-deployable molecular diagnostics in plant disease management (Paul et al., 2020).

Building on the traditional plant nucleic acid extraction method i.e., CTAB, molecular detection techniques such as polymerase chain reaction (PCR) and loop-mediated isothermal amplification (LAMP) have been widely applied for diagnosis of plant diseases like potato and tomato late blight. PCR-based methods provide high specificity but require complex experimental operations, high-standard laboratory environments, and well-trained personnel (Hieno et al., 2019; Khan et al., 2017; Ristaino et al., 2020; Zhen et al., 2016). LAMP assays, including colorimetric (Hansen et al., 2016) and PiSMC-targeting designs (Kong et al., 2020), enable faster detection but require relatively high isothermal temperatures (60-65 °C) and are prone to primer-dimer formation (Zhao et al., 2023). These limitations restrict the deployment of PCR and LAMP for rapid on-site diagnosis in agricultural fields.

Clustered regularly interspaced short palindromic repeats (CRISPR) and CRISPR-associated proteins (Cas) provide a powerful alternative to PCR and LAMP methods, owing to the programmability, sensitivity, specificity, and operational simplicity (Jiang et al., 2023; G. Liu et al., 2022; Weng et al., 2023). Cas12a and Cas13 proteins exhibit target-activated trans-cleavage activity, enabling specific and sensitive nucleic acid detection (Bai et al., 2019; Li et al., 2018; Liu et al., 2021). When coupled with isothermal amplification techniques such as recombinase polymerase amplification (RPA) (Wang et al., 2019, 2020), CRISPR/Cas systems have been successfully applied to virus (Fozouni et al., 2021; Kellner et al., 2019), bacteria (L. Liu et al., 2022; Wang et al., 2020; Xu et al., 2022), and parasitic pathogen detection (Li et al., 2022; Ma et al., 2021). Therefore, CRISPR-based detection is considered as a valuable approach for plant disease diagnosis deployable in the field.

In this study, we aim to develop a rapid, accurate and field-deployable diagnostic platform for early detection of *P. infestans*. To achieve this, we integrate polyvinyl alcohol (PVA) microneedle (MN)-based rapid DNA sampling with an isothermal RPA-CRISPR/Cas12a detection system and a smartphone-based fluorescence analyzer (Fig. 1). The MN patch is designed to enable fast and simplified nucleic acid extraction directly from infected leaves, while the RPA-CRISPR/Cas12a assay provides specific molecular recognition under isothermal conditions. Coupled with automated smartphone-based image acquisition and quantitative analysis, this integrated system enables a portable "sample-to-result" workflow for early-stage diagnosis of potato late blight in the field. This study provides a promising point-of-care diagnostic strategy for crop protection and disease management.

## 2. Materials and methods

The overall workflow of the integrated MN-RPA-CRISPR/Cas12a detection system is illustrated in Fig. 1. (1) DNA Extraction: a MN patch is pressed onto the potato leaf surface and then peeled off to extract pathogen DNA instantly in the field; (2) Detection Process: the extracted DNA is initially amplified by RPA, followed by CRISPR/Cas12a-mediated trans-cleavage of a fluorophore-quencher (FAM-BHQ1) reporter, generating a fluorescence signal which can be subsequently imaged with the mobile camera; (3) Result Visualization: fluorescent images are captured through a bandpass filter by a smartphone camera and the signals are processed automatically in real time with a homemade software.

### 2.1. Materials

All primers and crRNAs were synthesized by Sangon Biotech (Shanghai, China). LbCas12a protein and the reaction buffer were purchased from Sangon Biotech. The RPA kit was obtained from TwistDx Ltd. (Cambridge, Massachusetts, USA). DNA oligonucleotides were synthesized by Shanghai GeneBiogist Technology Co., Ltd. (Shanghai, China). CTAB extraction buffer was purchased from Solarbio (Beijing, China). Polydimethylsiloxane (PDMS) molds for MN fabrication were provided by Taizhou Microchip Medical Technology (Taizhou, China). Strains of *P. infestans*, *P. sojae*, and *P. capsici*, were obtained from the Laboratory of Fungicide Pharmacology & Pathogen Resistance, China Agricultural University.

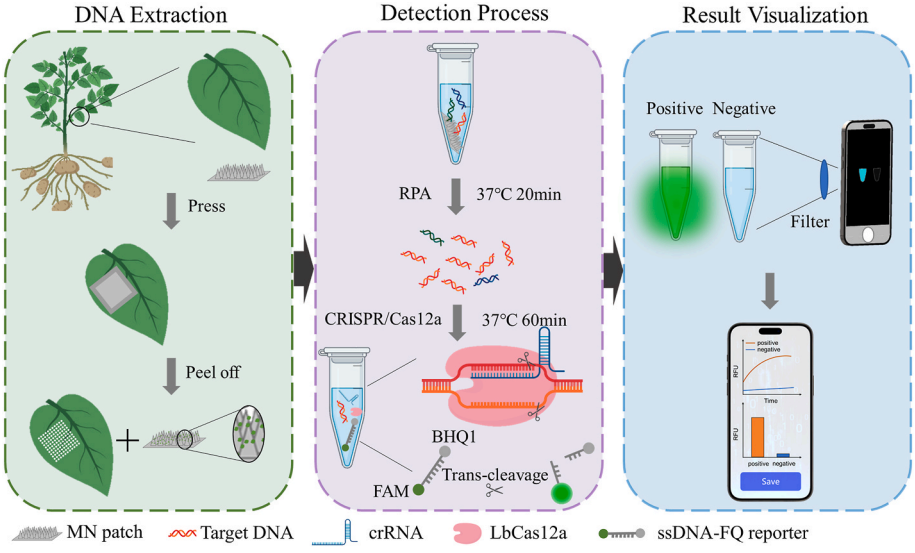



**Fig. 1.** Schematic illustration of the integrated RPA-CRISPR system for early-stage diagnosis of potato late blight, including MN-based DNA extraction, RPA-CRISPR/Cas12a detection, and smartphone-based fluorescence analyzer.

### 2.2. Microneedle patch fabrication

MN patches were fabricated as following procedures. A PDMS mold (13.3 mm × 13.3 mm) for MN fabrication contains a 15×15 array of conical cavities, and each cavity has 840 μm in depth, and provide a 280 μm diameter on the needle base. The PDMS mold was cleaned in an ultrasonic bath for 5 min, then dried and filled in with 500 μL of 15% (w/v) PVA solution (Paul et al., 2021b). To facilitate the sufficient infiltration of the PVA solution into the needle cavities, the mold was placed in a vacuum chamber for ~20 min to ensure the needle tips were completely filled. The mold was kept in the sealed chamber for an additional 15~20 min after the vacuum pump was off to dissipate the air bubbles from the PVA solution. Then the mold was left at room temperature for 24 h to dry off. The solidified MN patch can be carefully peeled off from the mold for use when dried. Each patch contains a 15×15 array of conical microneedles with 840 μm height and 280 μm base diameter. The fabricated MN patches were stored in sealed Petri dishes at room temperature.

### 2.3. DNA extraction with MN

The MN patches were fabricated with the method described above and then employed for *P. infestans* DNA extraction in the potato leaves (Fig. S1). For sampling, a fresh PVA-based MN patch was placed on the potato leaf surface with its microneedle tips facing downward. It was gently pressed with a finger to ensure the microneedles penetrated the leaf epidermis and disrupted plant cells. The patch was kept in contact with the leaf tissue for several seconds to facilitate sufficient absorption of the cell extract. Thereafter, the MN patch was carefully peeled off from the leaf surface. Subsequently, 50 μL of TE buffer (pH 8.0) was used to rinse the peeled patch for elution of the captured nucleic acids. Ultimately, the eluate was collected and stored at −20 °C for subsequent molecular analysis.

### 2.4. Establishment of RPA-CRISPR/Cas12a assay

Species-specific RPA primers and crRNA were designed targeting a unique genomic fragment of *P. infestans* (scaffold NW_003302563.1, positions 351~1400). Three forward and four reverse primers were screened by RPA followed by agarose gel electrophoresis, and the primer pair yielding the highest amplification efficiency (RPA-F3 and RPA-R1) was selected for subsequent experiments (Fig. S2). A 23 bp region containing a PAM site (TTTN-) within the RPA amplicon was selected as the CRISPR/Cas12a target site for crRNA design. Detailed information on primer and crRNA sequences, target site selection, and screening results is provided in Supporting Information 1.2 and Table S1.

The standard RPA reactions were performed using the TwistAmp Basic kit. Each 50 μL reaction contained one pellet, 29.5 μL of rehydration buffer, 480 nM each of forward and reverse primers, 2 μL DNA template, and 14 mM of magnesium acetate (MgOAc). The reaction mixture was incubated at 37 °C for 4 min, inverted 10 times, and centrifuged, and further incubated at 37 °C for 16 min.

The Cas12a-mediated trans-cleavage fluorescence detection (50 μL) consisted of 100 nM LbCas12a, 100 nM crRNA, 200 nM ssDNA-FQ reporter, 5 μL of reaction buffer, and 2 μL of RPA product. The ssDNA-FQ reporter was a non-specific single-stranded DNA probe that was labeled with a 6-FAM fluorophore (Ex 495 nm/Em 521 nm) at the 5′ end, and a BHQ1 quencher at the 3′ end. The reactions were incubated at 37 °C for 60 min in a QuantStudio 3 Real-Time PCR System (Thermo Fisher Scientific, Sunnyvale, CA, USA), with fluorescence measured every 5 min. All experiments were performed with three replicates.

### 2.5. Leaf inoculation in laboratory

Healthy potato leaves of similar size were selected and surface-sterilized by rinsing with tap water to remove dust, followed by washing with 75% ethanol and rinsing with sterile water. The leaves were then placed abaxial side up in Petri dishes on filter paper moistened with sterile water. *P. infestans* isolate VD4 was cultured on V8 agar medium, and zoospore suspensions were prepared as described in Supporting Information 1.3 and 1.4. Each leaf was evenly sprayed with 500 μL of *P. infestans* zoospore suspension at a concentration of $4 \times 10^4$ zoospores/mL. The Petri dishes were incubated in the dark at 18 °C (Vleeshouwers et al., 1999). After 24 h, residual droplets of the suspension were wiped off, and the leaves were flipped to keep the abaxial side down. All inoculated leaves were then transferred to room temperature and maintained under a 16-h light/8-h dark cycle for further incubation.

### 2.6. Design of the smartphone-based detection device

A low-cost, portable detection device integrating RPA isothermal amplification, CRISPR/Cas12a detection, and fluorescence readout with smartphone-based real-time analysis was developed. The device housing (20 cm × 12 cm × 17.4 cm; 450 g) was fabricated using through 3D printing with light-cured resin. The internal structure comprises the reaction zone, optical system, and temperature control unit. The reaction zone accommodated four 1.5 mL centrifuge tubes, allowing up to four parallel assays. Rectangular partitions (3.8 cm height; 1.5 cm width) were installed between adjacent reaction tubes to prevent fluorescence cross-interference. Heating was provided by a resistance wire heating pad mounted on the rear wall of the reaction zone, controlled by a temperature regulator to ensure stable incubation at 37 °C with real-time monitoring. Excitation was achieved by a 470 nm laser (50 mW) delivered via optical fibers (1.0 mm diameter) that vertically illuminated the bottom of each tube to excite FAM fluorophores. Fluorescence signals were directly captured by a smartphone camera through a 520 ± 15 nm bandpass filter, which blocked stray light and improved the signal-to-noise ratio. Both the temperature-controlled heating pad and the laser were powered by a portable power bank, enabling continuous operation up to 3 h, sufficient to complete the detection workflow. A custom-developed smartphone application was developed to automatically capture images every 5 min and generate fluorescence intensity curves, providing immediate result interpretation. The detailed information about the smartphone software and image processing procedure has been provided in Supporting Information 1.6 and Fig. S3, the original codes of the software has been uploaded to Github (https://github.com/moli59182-eng/fluo_app1).

## 3. Results and discussion

### 3.1. Efficiency of DNA extraction with MN

To compare the DNA extraction efficiency, DNA was isolated from *P. infestans*-infected potato leaves (6 days post-inoculation) using both MN patches and the CTAB approach (Supporting Information 1.1). In the MN approach, small fragments of potato leaf tissue adhered to the MN patch surface after puncture (Fig. 2d and e). The corresponding punctured leaf regions were then excised and processed using the CTAB method for direct comparison. DNA concentrations were measured using a NanoDrop One Microvolume UV-vis spectrophotometer.

MN patches yielded 50.2 ± 4.8 ng DNA (n = 5 replicates), whereas the CTAB method yielded 235.4 ± 15.3 ng DNA (n = 5 replicates) (Fig. 3a). The higher total DNA yield obtained with CTAB was primarily due to the larger mass of the sampled tissue (14 mg for CTAB vs. 0.9 mg for MN). When normalized by sample mass, the MN patches achieved a DNA yield of 56.3 ± 4.2 ng/mg compared to 18.1 ± 2.1 ng/mg for the CTAB method (Fig. 3b), indicating that MN extraction was more efficient compared to the traditional CTAB method. This result indicates that the MN patch provides efficient localized sampling and DNA recovery from a very small amount of plant tissue. The improved tissue-mass-normalized recovery may be attributed to the direct penetration

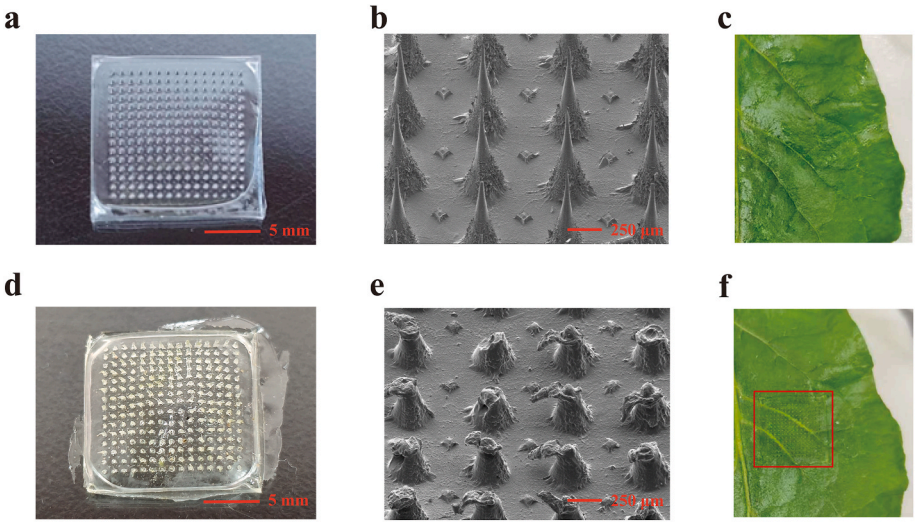



**Fig. 2.** Photograph and SEM image of the MN patch before (**a**, **b**) and after (**d**, **e**) leaf puncture. Images of potato leaves before (**c**) and after (**d**) punctured by the MN patch.

of the microneedles into leaf tissue, rapid dissolution of the PVA matrix, and close interfacial contact between the hydrated polymer and disrupted plant cells, which facilitates local DNA release and collection. In contrast to CTAB extraction, the MN method avoids grinding and homogenization steps, may help avoid extensive co-extraction of polysaccharides, polyphenols, and other plant-derived compounds that typically interfere with nucleic acid purification (Liang et al., 2015). Therefore, although CTAB extraction provides a higher absolute DNA amount, the MN-based method offers sufficient DNA recovery for RPA-CRISPR/Cas12a detection while substantially simplifying sample preparation and improving the tissue-mass-normalized extraction efficiency.

To verify that DNA extracted by the MN patches could be directly applied to downstream assays, unpurified and undiluted MN-extracted DNA was tested in both qPCR and RPA-CRISPR/Cas12a assays. For qPCR, primers targeting a 100 bp region of the *P. infestans* ITS gene (Paul et al., 2020b) were used. DNA extracted by the CTAB method served as a positive control, and DNA from healthy potato leaves served as a negative control. As shown in the amplification curves (Fig. 3c), *P. infestans* was successfully detected in both MN- and CTAB-extracted samples. Specifically, the Ct value for MN-extracted *P. infestans* DNA (24.7 ± 0.5) was higher than that of CTAB-extracted *P. infestans* (22.3 ± 0.3), consistent with its lower absolute concentration (Fig. 3d).

In the RPA-CRISPR/Cas12a assay, kinetic fluorescence curves (Fig. 3e) and endpoint fluorescence intensity values (Fig. 3f) demonstrated that the MN-extracted *P. infestans* DNA generated strong fluorescence signals ($2.1 \pm 0.1) \times 10^6$ RFU), significantly above the negative control ($4.6 \pm 0.2) \times 10^5$ RFU), indicating reliable detection of *P. infestans*. These findings suggest that *P. infestans* DNA extracted via MN patches is fully compatible with molecular assays and sufficient for direct pathogen detection, despite lower absolute yields compared with CTAB. Importantly, MN-extracted DNA can be directly used in qPCR and RPA-CRISPR/Cas12a assays without further purification, thereby greatly simplifying sample preparation and supporting rapid, field-deployable diagnosis.

### 3.2. RPA primer screening

To establish the RPA-CRISPR/Cas12a assay, a species-specific genomic fragment of *P. infestans* (position 351-1400 of scaffold NW_003302563.1) was selected as the target, and a corresponding crRNA was designed to recognize this region (Fig. S2a). The schematic illustrates the dsDNA target sequence (blue) and the complementary crRNA binding site (red). To ensure optimal amplification efficiency, multiple RPA primer combinations were evaluated using the RPA reaction system described in Supporting Information 1.2. The RPA amplification products were analyzed by 2% agarose gel electrophoresis. As illustrated in Fig. S2b and c, clear bands were observed for all primer combinations, the primer pair RPA-F3 (forward) and RPA-R1 (reverse) producing the strongest target bands and the highest amplification efficiency. These primers were therefore selected for subsequent assay development.

### 3.3. Sensitivity and specificity of the RPA-CRISPR/Cas12a assay

The detection sensitivity of the RPA-CRISPR/Cas12a assay was first evaluated using the recombinant plasmid PiNW. A 10-fold dilution series ($10^4$ to $10^{-2}$ pg/μL) was prepared, and 2 μL of each dilution was used as RPA template. Reactions were performed at 37 °C for 60 min with fluorescence measured every 5 min. Endpoint fluorescence intensity decreased proportionally with lower plasmid concentration, and no significant signal was observed below 0.01 pg/μL compared with the negative no-template control (Fig. 4a). The detection limit was determined to be 0.1 pg/μL (Fig. 4c). Linear regression analysis between log-transformed plasmid concentration and fluorescence intensity (Fig. 4e) yielded an $R^2$ value of 0.8991, confirming quantitative capability.

The detection sensitivity of the assay was further assessed using genomic DNA (gDNA) from *P. infestans* mycelium extracted using the CTAB method. A 10-fold dilution series ($10^4$ to $10^{-1}$ pg/μL) was prepared. Both endpoint and kinetic fluorescence analyze suggest a detection limit of ~2 pg/μL (Fig. 4b–d). Linear regression (Fig. 4f) showed an $R^2$ value of 0.9708, demonstrating excellent correlation. The higher detection limit for gDNA compared to the plasmid PiNW is likely attributed to the lower copy number of the target sequence per unit mass in the complex genomic DNA background. The analytical sensitivity achieved in this study is comparable to previously reported isothermal amplification assays for *P. infestans*. For example, Verma et al. (2019), Kong et al. (2020) and Paul et al. (2021) achieved detection limits of picogram-level using LAMP-based assays. Although these established amplification methods show similar analytical sensitivity, our assay integrates RPA amplification with CRISPR/Cas12a-mediated sequence-specific recognition and smartphone-based fluorescence readout. Therefore, the main advantage of the present method lies not only in its sensitivity, but also in the integration of minimally invasive MN sampling, rapid DNA release, isothermal amplification, CRISPR-based specificity, and portable readout for field-deployable early diagnosis of

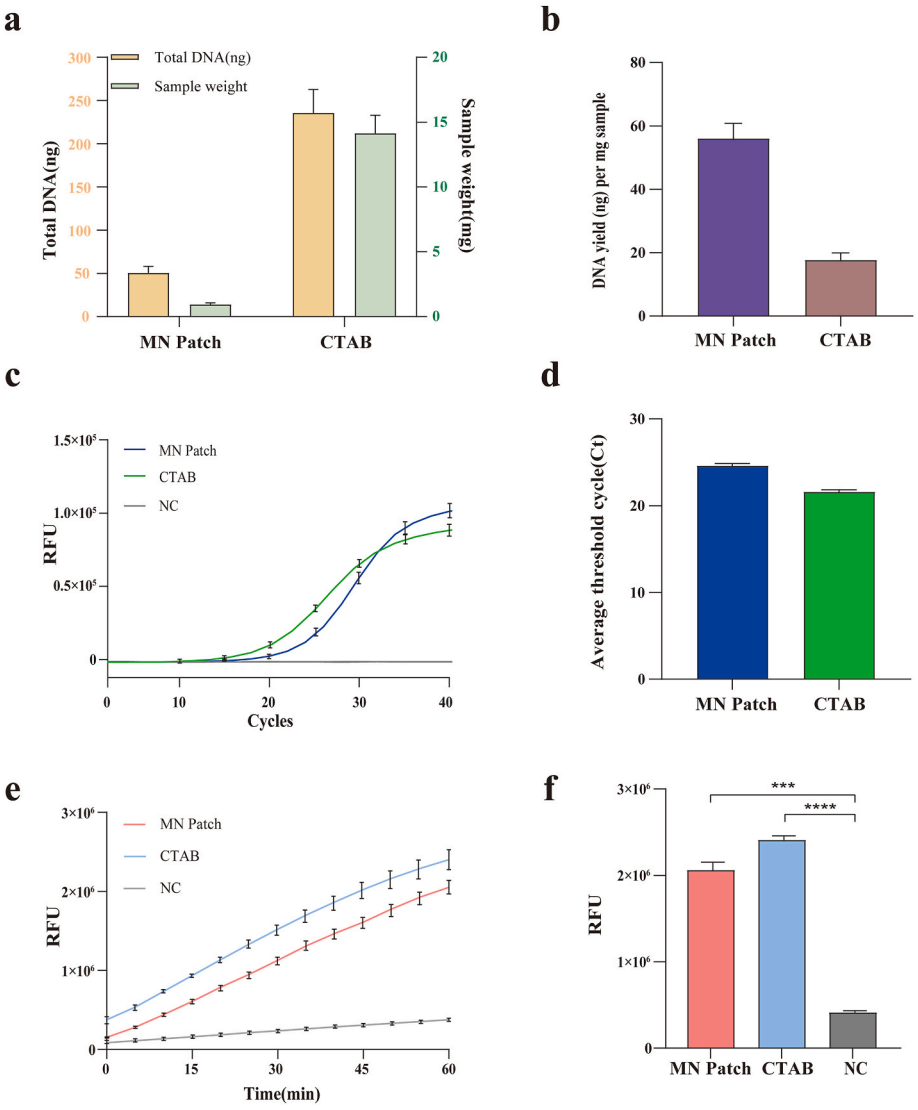



**Fig. 3.** Validation of MN patch-extracted DNA for direct use in molecular assays. **(a)** Total DNA yields (yellow) and sampling mass (green) for MN and CTAB methods. **(b)** DNA yield per mg of leaf tissue. Data are shown as mean ± SD (standard deviation, n = 5 replicates). **(c)** Real-time PCR amplification curves of DNA extracted by MN patches (50.2 ng/μL) and the CTAB method (235.4 ng/μL) from *P. infestans*-infected leaf tissues. **(d)** Ct values for MN- and CTAB-extracted DNA. Data are shown as mean ± SD (n = 3). **(e)** Kinetic fluorescence curves of the RPA-CRISPR/Cas12a assay using DNA extracted by MN patches (50.2 ng/μL) and the CTAB method (235.4 ng/μL). **(f)** Endpoint fluorescence intensity comparison between *P. infestans* DNA extracted by the MN patch and CTAB method. Data are shown as mean ± SD (n = 3). Statistical analysis: two-tailed Student's t-test; $^{*}P < 0.05$, $^{**}P < 0.01$, $^{***}P < 0.001$, and $^{****}P < 0.0001$; n.s.: not significant; NC: negative control. (For interpretation of the references to color in this figure legend, the reader is referred to the Web version of this article.)

potato late blight.

Specificity of the RPA-CRISPR/Cas12a assay was evaluated using gDNA extracted from *P. infestans*, *P. sojae*, and *P. capsici*, with sterile water as a negative control. As shown in Fig. 4g and h, only *P. infestans* gDNA triggered Cas12a activation and generated a detectable fluorescence signal, while no signal was observed with *P. sojae*, *P. capsici* or the negative control. These results demonstrate that the assay exhibits high specificity for *P. infestans*, without cross-reactivity to closely related oomycete species. This. high specificity is attributable to the combined stringency of the RPA primers and the crRNA design.

### 3.4. Early-stage detection of potato late blight

The ability of the MN-RPA-CRISPR/Cas12a platform to detect early *P. infestans* infection was evaluated with laboratory-inoculated potato leaves. A total of 20 leaves were inoculated, with an additional 5 uninoculated healthy leaves serving as negative controls. Specifically, from Day 1 to Day 5 post-inoculation, four independent inoculated leaves and one healthy leaf were evaluated each day. DNA was extracted from two separate sites on each leaf using MN patches with the same procedure, and sampling positions on both inoculated and healthy leaves were randomly selected to ensure unbiased representation. All samples were processed immediately for the RPA-CRISPR/Cas12a assay to diagnose the *P. infestans* infection.

During a 5-day monitoring period, uninoculated healthy leaves remained symptom-free, whereas laboratory-inoculated leaves began to develop visible late blight lesions on Day 4, which became more severer by Day 5 (Fig. 5a). Molecular detection using MN-extracted DNA revealed positive signals prior to symptom appearance. As shown in Fig. 5b, endpoint fluorescence intensities increased progressively from Day 2 onward, reflecting *P. infestans* pathogen accumulation in infected tissue. To distinguish positive samples from negative ones, a fluorescence threshold value was set as the mean signal of negative controls plus three times the SD (Mean + 3×SD), ensuring a false-positive rate below 0.15%. Negative sterile water controls (30 replicates) yielded a mean fluorescence intensity of ~$7.2 \times 10^5$ RFU with a SD of ~$0.8 \times 10^5$,

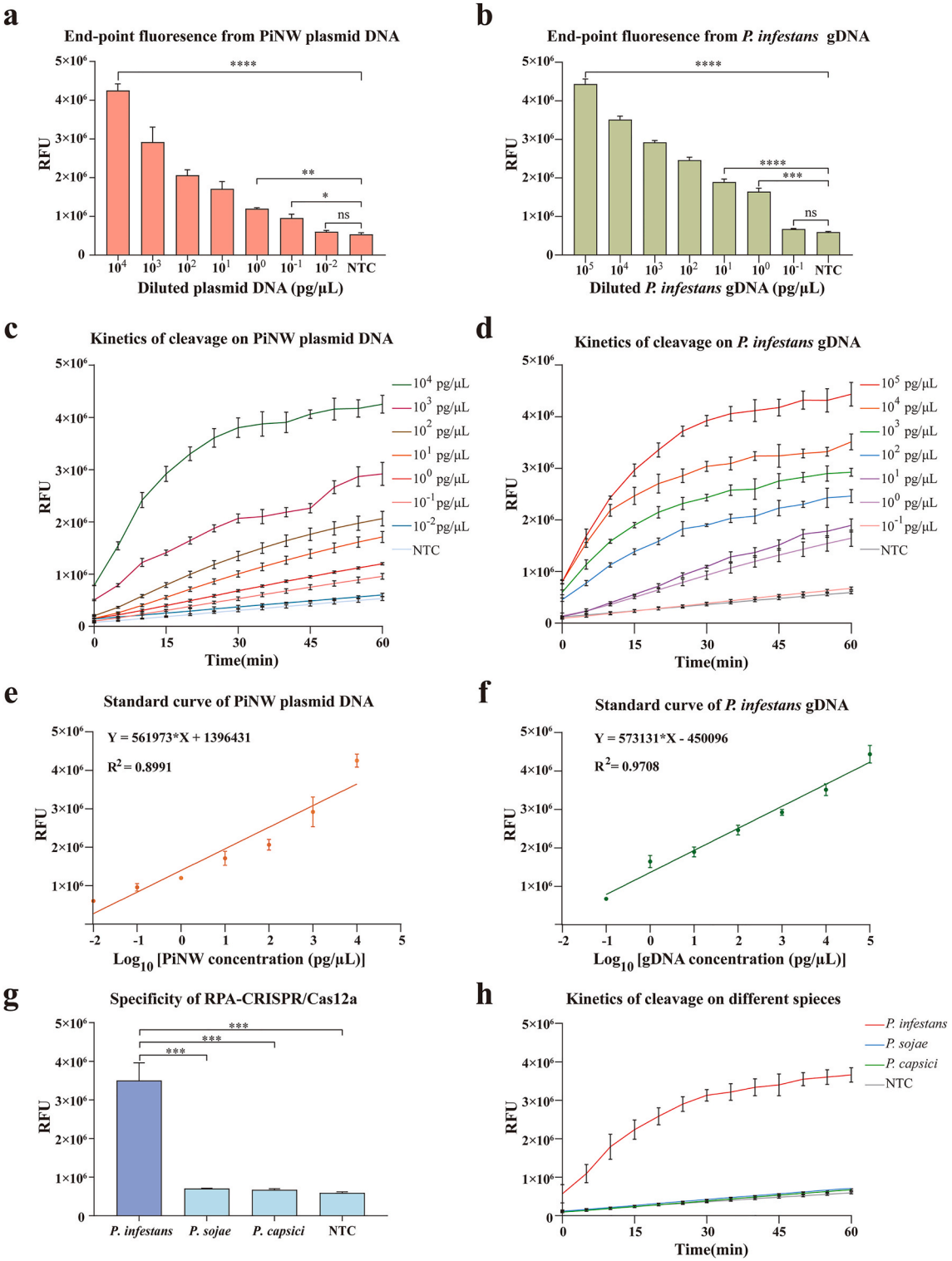



**Fig. 4.** Establishment of RPA-CRISPR/Cas12a assay. Sensitivity analysis with **(a, c, e)** plasmid PiNW and **(b, d, f)** *P. infestans* gDNA. **(g, h)** Specificity evaluation with *P. infestans* (positive control, 4.8 ng/μL), *P. sojae* (1.4 ng/μL), *P. capsici* (17.5 ng/μL) and NTC. Data are shown as mean ± SD from 3 replicates. Statistical analysis: two-tailed Student's t-test; $^{*}P < 0.05$, $^{**}P < 0.01$, $^{***}P < 0.001$, and $^{****}P < 0.0001$; n.s.: not significant; NTC: no-template control.

resulting in a calculated threshold of $9.6 \times 10^5$ RFU. This threshold effectively minimized false positives while ensuring reliable classification of infected samples. Applying this criterion, 3 of 8 inoculated samples were tested as positive on Day 2, 6 samples were positive on Day 3, and all were positive by Day 4 (Fig. 5b). The detection rate for each time point was defined as:

$$Detection\ rate = \frac{Number\ of\ positive\ samples}{Total\ number\ of\ samples\ tested} \times 100\%$$

The detection rate reached 100% on Day 4 post-inoculation, even though small portion of the leaves demonstrates visible symptoms (Fig. 5a–c). These results show that the MN-based DNA extraction

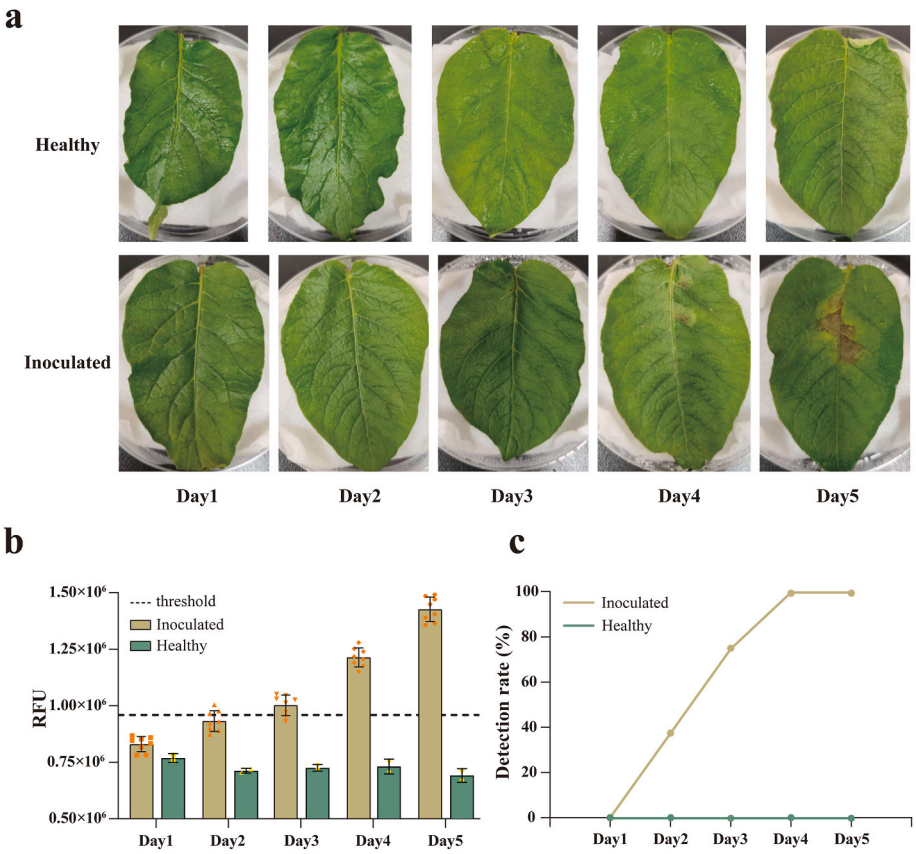



**Fig. 5.** Early detection of *P. infestans* using the MN-RPA-CRISPR/Cas12a system. **(a)** Time-course appearance of uninoculated healthy leaves (top) and laboratory-inoculated potato leaves (bottom) from Day 1-5 post-inoculation for symptom monitoring. **(b)** Endpoint fluorescence intensities across different inoculation days in laboratory-inoculated potato leaves (n = 8 samples/day, four independent leaves with two random sample sites on each) and uninoculated healthy leaves (n = 2 samples/day, one healthy leaf with two random sample sites). **(c)** Detection rate of *P. infestans* positive in laboratory-inoculated leaves and uninoculated healthy leaves on different inoculation days.

combined with the RPA-CRISPR/Cas12a enables early detection of potato late blight on Day 2 and Day 3 post inoculation, even before the visible symptoms developed on leaves, providing the advantage of pre-symptomatic diagnostic compared to conventional visual inspection.

### 3.5. Smartphone-coupled RPA-CRISPR detection system for POCT

To enable portable and field-deployable diagnosis, the RPA-CRISPR/Cas12a assay was integrated into a smartphone-based fluorescence detection device. The analytical performance of the device was first evaluated using serial dilutions ($10^4$ to $10^{-1}$ pg/μL) of *P. infestans* gDNA extracted by the CTAB method. For quantitative analysis, normalized fluorescence intensity was calculated as the change in signal during the reaction divided by the initial fluorescence intensity, as detailed in Supporting Information 1.6. Specifically, for each tube, the intensity value in the initial image captured by the smartphone software was recorded as the baseline, F0. The fluorescence intensity at each subsequent time point was normalized to its corresponding baseline according to (Ft − F0)/F0, where Ft represents the raw fluorescence intensity captured by the smartphone at time t. This tube-specific normalization minimizes the influence of tube position on the measured fluorescence signal, even when multiple tubes are analyzed simultaneously within the same smartphone image.

As shown in Fig. 6c–e, the smartphone-based detection device exhibited time-dependent fluorescence enhancement comparable to a benchtop PCR system. A strong linear relationship was observed between endpoint fluorescence intensity and the logarithm of DNA concentration, with a detection limit of ~4 pg/μL, demonstrating sensitivity equivalent to laboratory equipment.

To further validate field applicability, MN-extracted gDNA from late blight-infected potato leaves was tested directly on the smartphone device. As shown in Fig. 6g and h, infected samples produced clear fluorescence signals, while CTAB-extracted gDNA served as the positive control and sterile water as the negative control. Both endpoint images and normalized fluorescence intensities suggested that the integrated MN-RPA-CRISPR/Cas12a smartphone platform reliably detected *P. infestans* infection. Collectively, these results highlight the feasibility of a fully portable "sample-to-result" system for early and on-site detection of potato late blight.

## 4. Conclusions and perspectives

This study presents the CRISPR/Cas12a-based assay for the oomycete pathogen *P. infestans*, integrating MN sampling, isothermal RPA amplification, and smartphone-assisted fluorescence analysis into a portable "sample-to-result" platform. The assay achieved a limit of detection of 2 pg/μL for *P. infestans* gDNA with a benchtop real-time PCR system, and 4 pg/μL with the smartphone-integrated detection device, demonstrating analytical performance comparable to that of previously reported molecular diagnostic methods for *P. infestans*. High specificity was achieved through the combined recognition of species-specific RPA primers and crRNA targeting a unique genomic region of *P. infestans*, with no observable cross-reactivity toward the related *Phytophthora* species (*P. sojae* and *P. capsici*). In addition, the MN-based sampling strategy reduced the sample preparation time from 3 to 4 h for the CTAB method to 1 min, while exhibiting higher DNA extraction efficiency on a per-mass basis. The complete workflow was finished within 90 min at 37 °C using low-cost portable equipment, highlighting its potential for

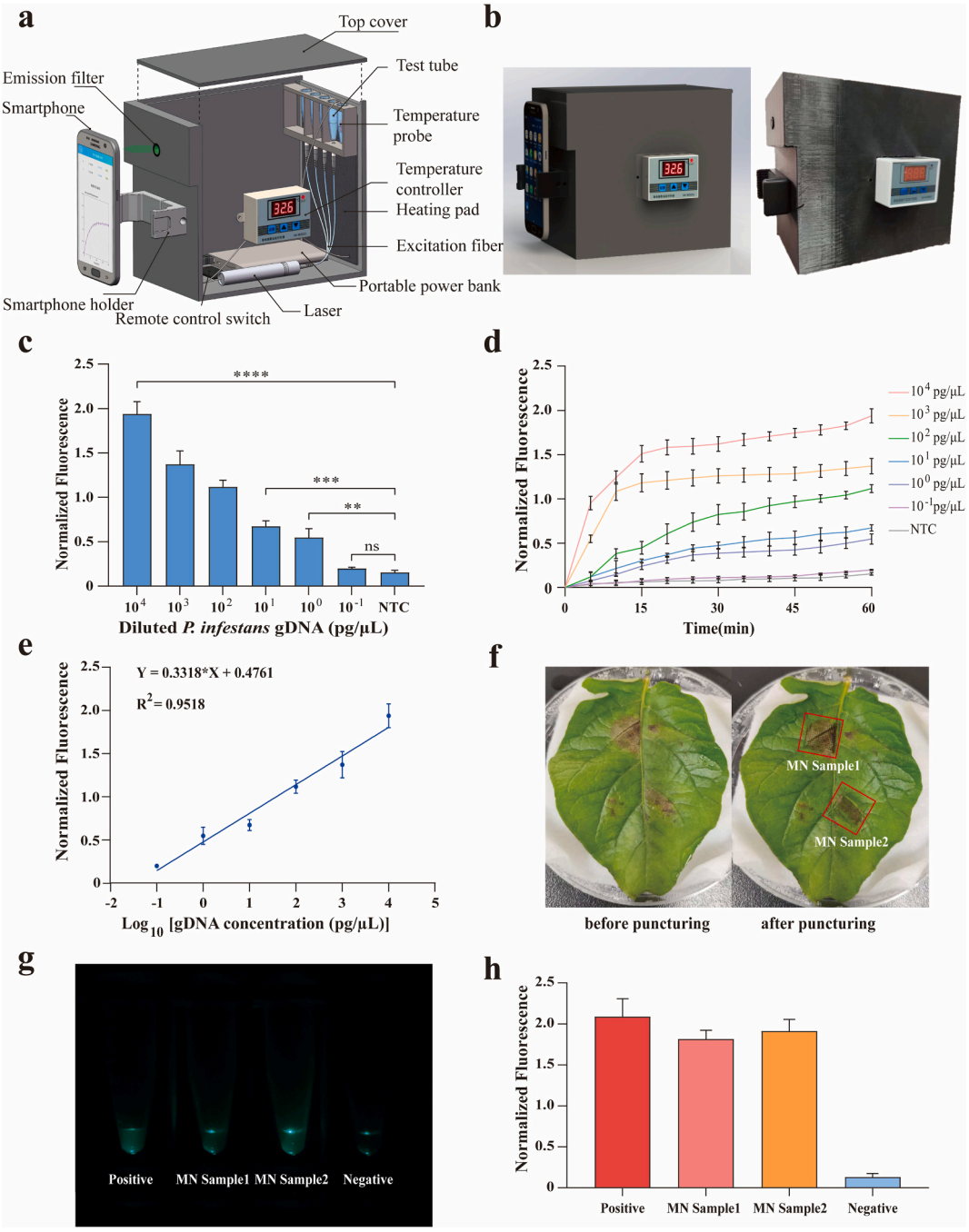



**Fig. 6.** Smartphone-integrated MN-RPA-CRISPR/Cas12a detection system. **(a)** Cross-sectional schematic of the smartphone reader. **(b)** Design diagram and photograph of the assembled device. **(c–e)** Sensitivity analysis using serial dilutions of *P. infestans* gDNA. Data are shown as mean ± SD (n = 6). **(f)** Representative photographs of a potato leaf before (left) and after (right) MN penetration. In the actual experiments, DNA was extracted from two separate sites on each leaf, and sampling was not restricted to visibly symptomatic regions. **(g)** Representative smartphone fluorescence images of assay results. **(h)** Normalized fluorescence intensities for infected, positive control, and negative control samples. Data are shown as mean ± SD (n = 3). Statistical analysis: two-tailed Student's t-test; $^{*}P < 0.05$, $^{**}P < 0.01$, $^{***}P < 0.001$, and $^{****}P < 0.0001$; n.s.: not significant; NTC: no-template control.

rapid and field-deployable molecular detection.

While the current platform already demonstrates promising practicality, several aspects remain to be further refined for broader deployment. In particular, systematic optimization of microneedle geometric parameters, including needle length, density, and array configuration, may provide additional gains in nucleic acid extraction efficiency. In addition, although the MN-based approach showed clear advantages over the CTAB method in terms of speed and per-mass extraction efficiency, future studies should further compare MN-assisted sampling with simple leaf collection followed by the same rapid extraction workflow. Furthermore, the development of lyophilized reagent formats may enhance storage stability and facilitate practical use under variable environmental conditions. Further evaluation under more diverse field settings would also help establish the robustness and adaptability of the platform for real-world applications.

Overall, this work provides a promising strategy for pre-symptomatic and field-deployable detection of potato late blight, and establishes a versatile framework for the rapid molecular diagnosis of other crop pathogens.

## Declaration of generative AI and AI-assisted technologies in the manuscript preparation process

During the preparation of this work, the authors used ChatGPT (openAI) for proofreading. The authors have reviewed and edited the output as needed and take full responsibility for the content of the published article.

## Funding

This work is supported by the National Natural Science Foundation of China (Award # 62401569, # 32471994) and the Natural Science Foundation of Shanghai Municipality (Award # 25ZR1402379).

## CRediT authorship contribution statement

**Jiangnan Zhao:** Investigation, Methodology, Writing – original draft. **Hanbo Xu:** Investigation, Software, Writing – original draft, Writing – review & editing. **Shifang Fei:** Investigation, Validation. **Cifu Xu:** Investigation, Software, Validation, Visualization. **Wenlong Yin:** Investigation. **Qingshan Wei:** Writing – review & editing. **Jianhan Lin:** Supervision, Writing – review & editing. **Gang Liu:** Conceptualization, Supervision, Validation. **Shilun Feng:** Writing – review & editing. **Fang Gao:** Conceptualization, Project administration, Supervision, Writing – original draft, Writing – review & editing. **Yan Wang:** Conceptualization, Project administration, Supervision, Writing – original draft, Writing – review & editing.

## Declaration of competing interest

The authors declare that they have no known competing financial interests or personal relationships that could have appeared to influence the work reported in this paper.

## Acknowledgements

The authors sincerely thank funding support from the National Natural Science Foundation of China (Award # 62401569 and # 32471994), the Natural Science Foundation of Shanghai Municipality (Award # 25ZR1402379). J. Lin, G. Liu and Y. Wang are supported by the 2115 Talent Development Program of China Agricultural University.

The authors also acknowledge Dingyuan Farm in Rizhao City, Shandong Province for providing samples of potato plants.

## Appendix A. Supplementary data

Supplementary data to this article can be found online at https://doi.org/10.1016/j.bios.2026.118943.

## Data availability

Data will be made available on request.

## References

Anderson, P.K., Cunningham, A.A., Patel, N.G., Morales, F.J., Epstein, P.R., Daszak, P., 2004. Emerging infectious diseases of plants: pathogen pollution, climate change and agrotechnology drivers. Trends Ecol. Evol. 19, 535–544. https://doi.org/10.1016/j.tree.2004.07.021.

Austin Bourke, P.M., 1964. Emergence of potato blight, 1843–46. Nature 203, 805–808. https://doi.org/10.1038/203805a0.

Bai, J., Lin, H., Li, H., Zhou, Y., Liu, J., Zhong, G., Wu, L., Jiang, W., Du, H., Yang, J., Xie, Q., Huang, L., 2019. Cas12a-Based On-Site and rapid nucleic acid detection of African swine fever. Front. Microbiol. 10, 2830. https://doi.org/10.3389/fmicb.2019.02830.

Fozouni, P., Son, S., Díaz De León Derby, M., Knott, G.J., Gray, C.N., D'Ambrosio, M.V., Zhao, C., Switz, N.A., Kumar, G.R., Stephens, S.I., Boehm, D., Tsou, C.-L., Shu, J., Bhuiya, A., Armstrong, M., Harris, A.R., Chen, P.-Y., Osterloh, J.M., Meyer-Franke, A., Joehnk, B., Walcott, K., Sil, A., Langelier, C., Pollard, K.S., Crawford, E. D., Puschnik, A.S., Phelps, M., Kistler, A., DeRisi, J.L., Doudna, J.A., Fletcher, D.A., Ott, M., 2021. Amplification-free detection of SARS-CoV-2 with CRISPR-Cas13a and Mobile phone microscopy. Cell 184, 323–333.e9. https://doi.org/10.1016/j.cell.2020.12.001.

Fry, W., 2008. *Phytophthora infestans*: the plant (and *R* gene) destroyer. Mol. Plant Pathol. 9, 385–402. https://doi.org/10.1111/j.1364-3703.2007.00465.x.

Fry, W.E., Birch, P.R.J., Judelson, H.S., Grünwald, N.J., Danies, G., Everts, K.L., Gevens, A.J., Gugino, B.K., Johnson, D.A., Johnson, S.B., McGrath, M.T., Myers, K.L., Ristaino, J.B., Roberts, P.D., Secor, G., Smart, C.D., 2015. Five reasons to consider *Phytophthora infestans* a reemerging pathogen. Phytopathology 105, 966–981. https://doi.org/10.1094/PHYTO-01-15-0005-FI.

Haas, B.J., Kamoun, S., Zody, M.C., Jiang, R.H.Y., Handsaker, R.E., Cano, L.M., Grabherr, M., Kodira, C.D., Raffaele, S., Torto-Alalibo, T., Bozkurt, T.O., Ah-Fong, A. M.V., Alvarado, L., Anderson, V.L., Armstrong, M.R., Avrova, A., Baxter, L., Beynon, J., Boevink, P.C., Bollmann, S.R., Bos, J.I.B., Bulone, V., Cai, G., Cakir, C., Carrington, J.C., Chawner, M., Conti, L., Costanzo, S., Ewan, R., Fahlgren, N., Fischbach, M.A., Fugelstad, J., Gilroy, E.M., Gnerre, S., Green, P.J., Grenville-Briggs, L.J., Griffith, J., Grünwald, N.J., Horn, K., Horner, N.R., Hu, C.-H., Huitema, E., Jeong, D.-H., Jones, A.M.E., Jones, J.D.G., Jones, R.W., Karlsson, E.K., Kunjeti, S.G., Lamour, K., Liu, Z., Ma, L., MacLean, D., Chibucos, M.C., McDonald, H., McWalters, J., Meijer, H.J.G., Morgan, W., Morris, P.F., Munro, C.A., O'Neill, K., Ospina-Giraldo, M., Pinzón, A., Pritchard, L., Ramsahoye, B., Ren, Q., Restrepo, S., Roy, S., Sadanandom, A., Savidor, A., Schornack, S., Schwartz, D.C., Schumann, U.D., Schwessinger, B., Seyer, L., Sharpe, T., Silvar, C., Song, J., Studholme, D.J., Sykes, S., Thines, M., Van De Vondervoort, P.J.I., Phuntumart, V., Wawra, S., Weide, R., Win, J., Young, C., Zhou, S., Fry, W., Meyers, B.C., Van West, P., Ristaino, J., Govers, F., Birch, P.R.J., Whisson, S.C., Judelson, H.S., Nusbaum, C., 2009. Genome sequence and analysis of the Irish potato famine pathogen *Phytophthora infestans*. Nature 461, 393–398. https://doi.org/10.1038/nature08358.

Hansen, Z.R., Knaus, B.J., Tabima, J.F., Press, C.M., Judelson, H.S., Grünwald, N.J., Smart, C.D., 2016. Loop-mediated isothermal amplification for detection of the tomato and potato late blight pathogen, *Phytophthora infestans*. J. Appl. Microbiol. 120, 1010–1020. https://doi.org/10.1111/jam.13079.

Hieno, A., Li, M., Afandi, A., Otsubo, K., Suga, H., Kageyama, K., 2019. Rapid detection of *Phytophthora nicotianae* by simple DNA extraction and real-time loop-mediated isothermal amplification assay. J. Phytopathol. 167, 174–184. https://doi.org/10.1111/jph.12785.

Hung, A.H., Rajesh, N.U., Bermudez, A., Boczek, S.M., Garcia-Marqués, F.J., Tan, Y.L., Hwang, J. (Luna), Sinawang, P.D., Ilyin, D., Jacobson, G.B., Demirci, U., Poplack, S. P., Pitteri, S.J., DeSimone, J.M., 2025. A microneedle device for rapid dermal interstitial fluid sampling. https://doi.org/10.1101/2025.03.13.641882.

Jiang, T., Hu, X., Lin, C., Xia, Z., Yang, W., Zhu, Y., Xu, H., Tang, H., Shen, J., 2023. Rapid visualization of *Clostridioides difficile* toxins A and B by multiplex RPA combined with CRISPR-Cas12a. Front. Microbiol. 14, 1119395. https://doi.org/10.3389/fmicb.2023.1119395.

Kellner, M.J., Koob, J.G., Gootenberg, J.S., Abudayyeh, O.O., Zhang, F., 2019. SHERLOCK: nucleic acid detection with CRISPR nucleases. Nat. Protoc. 14, 2986–3012. https://doi.org/10.1038/s41596-019-0210-2.

Khan, M., Li, B., Jiang, Y., Weng, Q., Chen, Q., 2017. Evaluation of different PCR-based assays and LAMP method for rapid detection of *phytophthora infestans* by targeting the Ypt1 gene. Front. Microbiol. 8. https://doi.org/10.3389/fmicb.2017.01920.

Kong, L., Wang, H., Wang, S., Xu, P., Zhang, R., Dong, S., Zheng, X., 2020. Rapid detection of potato late blight using a loop-mediated isothermal amplification assay. J. Integr. Agric. 19, 1274–1282. https://doi.org/10.1016/S2095-3119(19)62816-9.

Li, S., Wang, X., Yu, Y., Cao, S., Liu, J., Zhao, P., Li, J., Zhang, X., Li, X., Zhang, N., Sun, M., Cao, L., Gong, P., 2022. Establishment and application of a CRISPR-Cas12a-based RPA-LFS and fluorescence for the detection of *trichomonas vaginalis*. Parasit Vectors 15, 350. https://doi.org/10.1186/s13071-022-05475-5.

Li, S.-Y., Cheng, Q.-X., Liu, J.-K., Nie, X.-Q., Zhao, G.-P., Wang, J., 2018. CRISPR-Cas12a has both cis- and trans-cleavage activities on single-stranded DNA. Cell Res. 28, 491–493. https://doi.org/10.1038/s41422-018-0022-x.

Liang, Q., Gong, D., Wen, D., Deng, L., 2015. A valid measure to eliminate the influence of polysaccharides and polyphenols in recalcitrant longan (*Dimocarpus longan* L.) during DNA isolation. Afr. J. Biotechnol. 14, 2300–2306. https://doi.org/10.5897/ajb2015.14458.

Liu, G., Lin, Q., Jin, S., Gao, C., 2022. The CRISPR-cas toolbox and gene editing technologies. Mol Cell 82, 333–347. https://doi.org/10.1016/j.molcel.2021.12.002.

Liu, H., Wang, J., Zeng, H., Liu, X., Jiang, W., Wang, Y., Ouyang, W., Tang, X., 2021. RPA-Cas12a-FS: a frontline nucleic acid rapid detection system for food safety based on CRISPR-Cas12a combined with recombinase polymerase amplification. Food Chem. 334, 127608. https://doi.org/10.1016/j.foodchem.2020.127608.

Liu, L., Zhao, G., Li, X., Xu, Z., Lei, H., Shen, X., 2022. Development of rapid and easy detection of salmonella in food matrics using RPA-CRISPR/Cas12a method. LWT 162, 113443. https://doi.org/10.1016/j.lwt.2022.113443.

Ma, Q.-N., Wang, M., Zheng, L.-B., Lin, Z.-Q., Ehsan, M., Xiao, X.-X., Zhu, X.-Q., 2021. RAA-Cas12a-Tg: a nucleic acid detection System for *Toxoplasma gondii* based on CRISPR-Cas12a combined with recombinase-aided amplification (RAA). Microorganisms 9, 1644. https://doi.org/10.3390/microorganisms9081644.

Paul, R., Ostermann, E., Chen, Y., Saville, A.C., Yang, Y., Gu, Z., Whitfield, A.E., Ristaino, J.B., Wei, Q., 2021. Integrated microneedle-smartphone nucleic acid amplification platform for in-field diagnosis of plant diseases. Biosens. Bioelectron. 187, 113312. https://doi.org/10.1016/j.bios.2021.113312.

Paul, R., Ostermann, E., Gu, Z., Ristaino, J.B., Wei, Q., 2020. DNA extraction from plant leaves using a microneedle patch. Curr Protoc Plant Biol 5, e20104. https://doi.org/10.1002/cppb.20104.

Ristaino, J.B., Saville, A.C., Paul, R., Cooper, D.C., Wei, Q., 2020. Detection of *Phytophthora infestans* by loop-mediated isothermal amplification, real-time LAMP, and Droplet digital PCR. Plant Dis. 104, 708–716. https://doi.org/10.1094/PDIS-06-19-1186-RE.

Verma, G., Sharma, S., Raigond, B., Pathania, S., Naga, K., Chakrabarti, S.K., 2019. Development and application of fluorescent loop mediated isothermal amplification technique to detect *Phytophthora infestans* from potato tubers targeting ITS-1 region. 3 Biotech 9, 345. https://doi.org/10.1007/s13205-019-1878-2.

Vleeshouwers, V.G.A.A., Van Dooijeweert, W., Keizer, L.C.P., Sijpkes, L., Govers, F., Colon, L.T., 1999. A laboratory assay for *Phytophthora infestans* resistance in various solanum species reflects the field situation. Eur. J. Plant Pathol. 105, 241–250.

Wang, B., Wang, R., Wang, D., Wu, J., Li, J., Wang, J., Liu, H., Wang, Y., 2019. Cas12aVDet: a CRISPR/Cas12a-Based platform for rapid and visual nucleic acid detection. Anal. Chem. 91, 12156–12161. https://doi.org/10.1021/acs.analchem.9b01526.

Wang, Y., Ke, Y., Liu, W., Sun, Y., Ding, X., 2020. A one-pot toolbox based on Cas12a/crRNA enables rapid foodborne pathogen detection at attomolar level. ACS Sens. 5, 1427–1435. https://doi.org/10.1021/acssensors.0c00320.

Wang, Z., Tong, S., Niu, J., Cao, C., Gao, A., Jiao, Y., Fu, Y., Li, D., Pan, X., Cui, D., Sheng, N., Yan, L., Cui, S., Lin, S., Liu, Y., 2025. Microneedles: multifunctional devices for drug delivery, body fluid extraction, and bio-sensing. Nanoscale 17, 740–773. https://doi.org/10.1039/D4NR03538K.

Weng, Z., You, Z., Yang, J., Mohammad, N., Lin, M., Wei, Q., Gao, X., Zhang, Y., 2023. CRISPR-cas biochemistry and CRISPR-Based molecular diagnostics. Angew. Chem. Int. Ed. 62, e202214987. https://doi.org/10.1002/anie.202214987.

Wu, M., Liu, L., 2026. Microneedles biosensors for disease diagnosis: from fabrication to AI enhancement. TrAC, Trends Anal. Chem. 197, 118731. https://doi.org/10.1016/j.trac.2026.118731.

Xu, J., Ma, J., Li, Y., Kang, L., Yuan, B., Li, S., Chao, J., Wang, L., Wang, J., Su, S., Yuan, Y., 2022. A general RPA-CRISPR/Cas12a sensing platform for *Brucella spp.* detection in blood and milk samples. Sens Actuators B Chem 364, 131864. https://doi.org/10.1016/j.snb.2022.131864.

Zhao, Z., Wang, S., Dong, Z., Fan, Q., Lei, R., Kuang, R., Zhang, Y., 2023. One-Step reverse-transcription recombinase-aided amplification CRISPR/Cas12a-Based lateral flow assay for fast field screening and accurate differentiation of four major tobamoviruses infecting tomato and pepper. J Agric Food Chem acs.jafc.3c05268. https://doi.org/10.1021/acs.jafc.3c05268.

Zhen, Z., Zhang, M., Yu, Y., Gao, X., Zhu, Y., Yan, Y., Zhang, R., 2016. Establishment of a loop-mediated isothermal amplification (LAMP) detection method for genetically modified maize MON88017. Eur. Food Res. Technol. 242, 1787–1793. https://doi.org/10.1007/s00217-016-2678-0.

Zheng, B., Li, Q., Fang, L., Cai, X., Liu, Y., Duo, Y., Li, B., Wu, Z., Shen, B., Bai, Y., Cheng, S.-X., Zhang, X., 2024. Microorganism microneedle micro-engine depth drug delivery. Nat. Commun. 15, 8947. https://doi.org/10.1038/s41467-024-53280-8.

Zheng, M., Sheng, T., Yu, J., Gu, Z., Xu, C., 2024. Microneedle biomedical devices. Nat. Rev. Bioeng. 2, 324–342. https://doi.org/10.1038/s44222-023-00141-6.